Design of Zeeman Slower for Strontium atoms

A thesis submitted towards partial fulfilment of
BS-MS Dual Degree Programme

by

Sindhu Jammi

under the guidance of

Dr. Umakant Rapol

Assistant Professor

Indian Institute of Science Education and Research
Pune

Certificate

This is to certify that this thesis entitled "Design of Zeeman Slower for Strontium atoms" submitted towards the partial fulfilment of the BS-MS dual degree programme at the Indian Institute of Science Education and Research Pune represents original research carried out by "Sindhu Jammi" at the "Indian Institute of Science Education and Research, Pune", under the supervision of "Dr. Umakant Rapol" during the academic year 2012-2013.

Student
Sindhu Jammi

Supervisor
Dr. Umakant
Rapol

Acknowledgements

I would like to thank my guide, Dr. Umakant Rapol for the opportunity to work in his lab for this project. I am grateful to him for his help in all aspects of the project and I have learnt a lot working with him.

I thank my colleagues in the lab, Md. Noaman, Sunil Kumar and Sumit Sarkar for the discussions we have had and their help with my work. I thank them and my other colleagues Gunjan Verma, Tomin James and Chetan Vishwakarma for providing a very friendly and encouraging atmosphere in the lab. I would also like to thank Mr. Prashant Kale and Mr. Nilesh Dumbre for their technical assistance with my experiment.

I thank my parents for all their support throughout my education.

Abstract

The properties of a collection of atoms at extremely low temperatures (of the order of micro-kelvins or lesser) have been of theoretical interest for decades. It is only with the relatively recent advent of laser cooling has it been possible to create the conditions in which these properties can be studied. Laser cooling can decrease the temperature of atoms from around 900 K to a few microKelvins. The atoms experience a retarding force as they travel in a laser beam as they absorb and emit photons traveling in the opposite direction. There will be a Doppler shift in the velocity of the atoms due to this and the atoms move out of the range of the frequency of the light beam. One of the ways to correct for this is the design for a Zeeman Slower. The Zeeman Slower comprises a laser beam and a magnetic field in a solenoid. A Zeeman Slower for Strontium atoms has been designed as part of this project. The wavelength of the laser beam used is 461 nm and it addresses the $^1S_0$ to $^1P_1$ transition of the atoms. This transition has a relatively large line-width of 32 MHz and using this can achieve high cooling rates. The Zeeman effect due to the magnetic field in the solenoid shifts the levels of the atoms. A spatially varying magnetic field profile can be designed to make sure that the energy gap between the two levels remains in tune with the frequency of the laser (i.e. the atoms will still be able to absorb the photons). The Slower can reduce the velocity of the atoms to a few tens of m/s. The atoms will then be loaded in a Magneto-Optical Trap which consists of six orthogonal beams intersecting to slow the atoms and a weak magnetic trap to push the atoms into a small sphere and trap them. Another way to load atoms into a MOT is to use a 2D MOT as a source of a collimated beam of slowed atoms. It is loaded in a vapour cell and the output is a beam of atoms which travels to the 3D MOT chamber. This configuration consists of four laser beams orthogonal to the axis of propagation to slow down atoms and four coils producing a weak magnetic field to push the atoms towards the axis. The 2D MOT uses the 461 nm transition and the 3D MOT uses the $^1S_0$ to $^3P_1$ transition of wavelength 689 nm. The output flux of both the sources can be compared. The advantages and disadvantages of the two techniques are discussed.

Contents

Chapter 1

Introduction

1.1 History

The proposal to use radiation scattering forces on atoms to slow them down was first made by Wineland and Dehmelt [1] and Hansch and Schawlow [2] when they recognized the fact that this force would be dependent on the velocity of the atoms. One simple implementation of this idea is to send a stream of atoms into a light beam with a wavelength that addresses a transition from a lower to higher state. Early experiments were conducted by Phillips and Metcalf [3], Chu and Wieman [4], and Meystre [5] resulting in the successful slowing and thereby cooling of atoms to a few hundredths of a Kelvin.

As the atoms decelerate, the Doppler shift takes the laser frequency out of resonance with the atomic frequency. There are two ways that this problem is dealt with. Phillips [3] and Pritchard [6] introduced a spatially varying magnetic field along the path of the atoms such that the change in the atomic frequency due to the Zeeman effect of the magnetic field compensates for the change in Doppler shift. Another method introduced by Phillips [7], Zhu [8] and Wieman [9] is to change the laser frequency to keep in resonance with the changing atomic frequency.

The optical molasses state achieved by the intersection of six laser beams so that the atoms experience viscous damping in whatever direction they move has been theorized by Dalibard, Phillips [10] and Ashkin [11], and experimentally shown by Phillips [12] and Wieman [13]. The concept of Sisyphus cooling (that goes beyond the Doppler limit) has been explained by Dalibard and Cohen-Tannoudji [14]. In about ten years (1979-1989), Laser cooling has brought down the temperature of atoms from a few hundredths of a Kelvin to a few micro Kelvins.

1.2 Motivation for Laser cooling of Strontium

Alkaline-earth metals have many features not present in alkali systems that can be exploited for experiments in various fields like precision metrology, quantum information processing and quantum many body physics. The two valence electrons give rise to electronic properties that are significantly different from conventional alkali metal systems.

Some of the unique properties of Strontium are the four naturally occurring stable isotopes (both Bosonic and Fermionic), a ground state without electronic magnetic moment, the very strong $^1S_0 - {}^1P_1$ transition at 461 nm that is good for laser cooling, the narrow inter-combination transition $^1S_0 - {}^3P_1$ that has a Doppler limit three orders of magnitude lesser than the other $^1S_0 - {}^3P_0$ that arises in the fermionic ^{87}Sr isotope due to hyperfine interactions. The narrow inter-combination lines and the metastable states associated with them offer very good possibilities for laser cooling. Strontium also has a wide range of inter-isotopic scattering lengths that are useful in the investigation of fundamental laws. Apart from studying the properties of ultracold atoms, Strontium is also used in the study of ultra cold molecules, both homogeneous and heterogeneous. Strontium molecules are formed by photoassociative spectroscopy of atoms in optical lattices, and Strontium - Rubidium molecules having both magnetic and electric dipole moment are used in the study of many body physics.

The primary standard of time at present is set by the Caesium atomic clock. One second is defined as the duration of 9,192,631,770 periods of the radiation corresponding to the transition between the two hyperfine levels of the ground state of the Caesium 133 atom. The accuracy of this definition lies in the universality of the atomic transition frequencies as opposed to the definition of a second as 1 in 86,400 parts of a mean solar day (as it does not account for irregularities in the rotation of the Earth). The transition used to probe the Caesium atoms is a microwave transition operating at 9.2×10^9 Hz. The principle of operation of atomic clocks is that an external source is locked in resonance with the atomic transition that is to be probed. However, there is an inherent uncertainty in finding out the actual frequency ν_0 that broadens the width of the resonance $\delta\nu$. The stability of the clocks depends on the quality factor $Q = \nu_0/\delta\nu$. The deviation of the clock is inversely proportional to the quality factor and the life-time of the upper state τ. The fractional uncertainty given by the term $\frac{1}{Q\tau\sqrt{N_{at}}}$ of the Caesium clocks is 10^{-15}, meaning that the deviation of these clocks would be less than a second in 10^7 years.

Working with higher frequencies improves the quality factor of the clocks thereby increasing their stability, when all the other factors are equal. For

example, Strontium clocks operate at an optical frequency of 4.3×10^{14} Hz. The transition probed is the ${}^1S_0 - {}^3P_0$ transition that has an extremely narrow linewidth < 1 mHz. Many systematic corrections do not depend on the frequency used for probing. Thus the fractional stability increases directly with the increase of the frequency used. The magnitude of the frequency used in optical clocks is 4-5 orders larger than that used in standard Caesium clocks. Thus, Strontium clocks are already more accurate than the present standard of time. But the Doppler shift is directly proportional to the velocity of atoms. This implies that to improve accuracy, we need to reduce the velocity of atoms as much as possible. Here, laser cooling comes into the picture. Both neutral atoms and ions can be used as an atomic reference. Stability also increases as $1/\sqrt{N}$ where N is the number of atoms being probed as this reduces the inherent statistical uncertainties. Using ions is a limitation as we can probe only one ion at a time (probing two ions together destabilizes the system with the Coulomb interactions). But using neutral atoms present no problems of this kind. Many neutral atoms can be probed together by trapping them in a periodic potential like an optical lattice. The optical lattice clocks can improve the accuracy by at least an order of magnitude over the optical clocks. The fractional accuracy of the optical lattice clocks is calculated to be 10^{-18} which means that the deviation would be less than a second in about 10^{10} years which is roughly the age of the Universe.

The proposals for the optical clocks had to overcome two problems. It is not possible to probe the higher frequencies of the transition using electronic cycle counters. The design of optical frequency combs which connect the optical clocks to the electronic counters surmounted this problem [15]. The second obstacle was that the optical fields used to trap the atoms would induce an ac Stark shift that changes the clock frequencies depending on the local intensity of the lasers. However, it has been found that using a 'magic' wavelength for the trapping potentials removes the differential effect of the optical fields as it shifts the two levels required by the same amount [16]. The proposal outlining the idea of the Strontium clock was made by Katori in 2003 [17] and the magic wavelength required was determined by Katori and Takamoto in the same year [18]. The clock was experimentally realized in three different laboratories by Takamoto [19], Le Targat [20] and Ludlow [21] in 2006.

The accuracy of Strontium optical lattice clocks would lead to many advances in fundamental science like redefining the second and mapping Earth's gravity using the gravitational redshift. Also possible are reproducible tests of Einstein equivalence principle [22], the coupling of fundamental constants to gravity [23] and the time variation of fundamental constants. Technologies that use global positioning systems and broadband communication networks

also benefit from the more precise measurement of time.

To achieve a Strontium optical lattice clock, the atoms are to be cooled down and trapped in a magnetic or optical dipole trap and from there loaded into an optical lattice. The clock transitions will be probed in the lattice. In this project, I have designed a Zeeman Slower for the first stage of cooling required for the atoms. I have also compared the efficiency of loading atoms from a Zeeman Slower to that of loading atoms from a 2D Magneto-Optical Trap, another source of a collimated beam of slow atoms. I have compared the different experimental aspects of the two systems. I have also discussed two kinds of oven collimation systems from which the atoms enter first stage of cooling.

1.3 Overview of the thesis

The thesis is divided into four parts. In the second chapter (the Theory), the first two sections give the fundamentals of light matter interaction and the cooling and trapping mechanisms of atoms. The third section explains the operating principles of the 2D MOT to the 3D MOT system and gives a theoretical model for the output flux of the 2D MOT. The fourth section discusses an oven collimation system. The fifth section is about the Strontium atomic system and mentions all the things required for the laser cooling of these atoms. The third chapter (Experiment) gives all the basic calculations required for designing the Zeeman Slower and explains how the magnetic field is simulated to finalize different parameters. The results chapter gives the data collected for the experimentally measured magnetic field and the expected output flux. The fifth chapter (the discussion) compares various aspects of the Zeeman Slower and the 2D MOT system, another oven collimation system with the previous one and gives the future plan.

Chapter 2

Theory

2.1 Interaction of atoms with Radiation

The interaction of a two-level atom with radiation is described using a semi-classical treatment, i.e. the radiation is treated as a classical electric field and the atom is treated quantum mechanically. We start with the time dependent Schrodinger equation

$$i\hbar\frac{\partial\Psi}{\partial t} = \hat{H}\Psi \tag{2.1}$$

The Hamiltonian $\hat{H}$ has two parts, the unperturbed Hamiltonian $\hat{H}_0$ and the interaction with the electric field which is dependent on time $\hat{H_1}(t)$.

$$\hat{H} = \hat{H}_0 + \hat{H_1}(t) \tag{2.2}$$

The unperturbed eigenvalues and eigenfunctions are the atomic energy levels E_1 and E_2, and the wavefunctions ψ_1 and ψ_2. The wavefunction of the total Hamiltonian $\hat{H}$ can be written as a function of these eigenvalues and eigenfunctions.

$$\Psi(\vec{r},t) = c_1(t)\psi_1(\vec{r})e^{-iE_1t/\hbar} + c_1(t)\psi_2(\vec{r})e^{-iE_2t/\hbar}. \tag{2.3}$$

Taking $\omega_i = E_i/\hbar$ and writing the above equation in the Dirac ket notation, we get

$$\Psi(\vec{r},t) = c_1|1\rangle e^{-i\omega_1 t} + c_2|2\rangle e^{-i\omega_2 t} \tag{2.4}$$

As the equation should be normalized, the time dependent coefficients c_1 and c_2 should satisfy

$$|c_1|^2 + |c_2|^2 = 1 \tag{2.5}$$

2.1.1 Bloch sphere treatment

In the Bloch sphere representation, the two levels of the atoms $|1\rangle$ and $|2\rangle$ are taken to be the bottom and top points of a sphere of radius one unit. The superposition states of the two levels lie on the surface of the sphere and are given by the equation

$$|\psi\rangle = c_1|1\rangle + c_2|2\rangle$$

with the normalization condition being $|c_1|^2 + |c_2|^2 = 1$. The direction of the Bloch vectors describing the superposition states can be written in the Cartesian coordinates (x, y, z) or in the spherical polar coordinates (r, θ, ϕ) with

$$\begin{aligned} x &= r\sin\theta\cos\phi, \\ y &= r\sin\theta\sin\phi, \\ z &= r\cos\theta, \\ r^2 &= x^2 + y^2 + z^2 \end{aligned}$$

We can find out the behaviour of a two-level system (like the populations in the two states) by calculating the electric dipole moment induced in the atom due to the external electric field using the Bloch sphere representation (as given in the book Atomic Physics by C.J. Foot). The electric field is taken to be along $\hat{e_x}$ and the component of the dipole along this direction is given by calculating the expectation value [24]

$$-eD_x(t) = -\int \Psi^\dagger(t) ex \Psi(t) d^3\vec{r} \tag{2.6}$$

This implies that the required dipole moment is given by

$$D_x(t) = \int (c_1 e^{-iw_1 t}\psi_1 + c_2 e^{-iw_2 t}\psi_2)^* x (c_1 e^{-iw_1 t}\psi_1 + c_2 e^{-iw_2 t}\psi_2) d^3\vec{r} \tag{2.7}$$

$$= c_2^* c_1 X_{21} e^{iw_0 t} + c_1^* c_2 X_{12} e^{-iw_0 t}. \tag{2.8}$$

where $\omega_0 = \omega_2 - \omega_1$ and $X_{12} = \langle 1|x|2\rangle$.

As $X_{21} = X_{12}^*$ and $X_{11} = X_{22} = 0$, we see that the dipole moment is a real quantity. The terms $c_1^* c_2$ and $c_2^* c_1$ are the coherences of the system. They are the off-diagonal elements of the density matrix whereas the diagonal elements are the populations. The density matrix is given by

$$|\Psi\rangle\langle\Psi| = (c_1 c_2)^T (c_1^* c_2^*) \tag{2.9}$$

When the frequency of the radiation is not at the atomic resonance, we define new variables $\bar{c_1}$ and $\bar{c_2}$ as

$$\bar{c_1} = c_1 e^{-i\delta t/2} \tag{2.10}$$

$$\bar{c_2} = c_2 e^{i\delta t/2} \tag{2.11}$$

with $\delta = \omega - \omega_0$ where ω is the frequency of the laser.

This does not affect the populations of the levels, but the coherences change as $\bar{\rho_{12}} = \rho_{12} exp(-i\delta t)$ and $\bar{\rho_{21}} = \rho_{21} exp(i\delta t)$. The dipole moment in terms of these coherences is

$$-eD_x(t) = -eX_{12}\rho_{12}e^{i\omega_0 t} + \rho_{21}e^{-i\omega_0 t} \tag{2.12}$$

$$= -eX_{12}\bar{\rho_{12}}e^{i\omega t} + \bar{\rho_{21}}e^{-i\omega t} \tag{2.13}$$

$$= -eX_{12}(u\cos\omega t - v\sin\omega t) \tag{2.14}$$

where u and v are the in-phase and quadrature components of the dipole in a frame rotating at ω and are given by

$$u = \bar{\rho_{12}} + \bar{\rho_{21}} \tag{2.15}$$

$$v = -i(\bar{\rho_{12}} - \bar{\rho_{21}}) \tag{2.16}$$

To find out the time derivatives of c_1 and c_2, we substitute the expression for the wavefunction in the time-dependent Schrodinger equation to get

$$i\dot{c_1} = \Omega\cos(\omega t)e^{-i\omega_0 t}c_2 \tag{2.17}$$

$$i\dot{c_2} = \Omega^*\cos(\omega t)e^{i\omega_0 t}c_1 \tag{2.18}$$

where Ω, the Rabi frequency is given by

$$\Omega = \frac{e}{\hbar}\int \psi_1^*(r)\vec{r}\vec{E}_0\psi_2(r)d^3\vec{r} \tag{2.19}$$

with the electric field $\vec{E} = |\vec{E_0}|\hat{e_x}\cos(\omega t)$.

Writing $\cos(\omega t)$ in terms of exponentials, we get

$$i\dot{c_1} = c_2 e^{i(\omega-\omega_0)t} + e^{-i(\omega+\omega_0)t}\frac{\Omega}{2} \tag{2.20}$$

$$i\dot{c_2} = c_1 e^{i(\omega+\omega_0)t} + e^{-i(\omega-\omega_0)t}\frac{\Omega}{2} \tag{2.21}$$

The term with $\omega + \omega_0$ oscillates much faster than the term with $\omega - \omega_0$ and averages to zero over typical interaction times. Thus it can be neglected

compared to the other term. This is the rotating wave approximation and using it, we can write

$$i\dot{c_1} = c_2 e^{i\delta t}\Omega/2 \tag{2.22}$$

$$i\dot{c_2} = c_1 e^{-i\delta t}\Omega/2 \tag{2.23}$$

From these equations, the time derivatives of ρ_{22}, $\dot{\rho_{12}}$ and $\dot{\rho_{21}}$ can be calculated. These equations in terms of u and v are

$$\dot{u} = \delta v \tag{2.24}$$

$$\dot{v} = -\delta u + \Omega(\rho_{11} - \rho_{22}) \tag{2.25}$$

$$\dot{\rho_{22}} = \Omega v/2 \tag{2.26}$$

Writing these equations more concisely (by taking $w = \rho_{11} - \rho_{22}$),

$$\dot{u} = \delta v \tag{2.27}$$

$$\dot{v} = -\delta u + \Omega w \tag{2.28}$$

$$\dot{w} = -\Omega v \tag{2.29}$$

With these equations, the populations of the states can be found out in a steady state.

2.1.2 The Optical Bloch equations

The energy of a two-level atom is proportional to the population of the excited state, $E = \rho_{22}\hbar\omega_0$. To account for spontaneous emission in the system, we treat it as a damped classical harmonic oscillator [24].

The equation of motion for a harmonic oscillator of natural frequency ω_0 with the driving frequency ω is

$$\ddot{x} + \beta\dot{x} + \omega_0^2 x = F\cos\omega t/m \tag{2.30}$$

Taking an ansatz of the form

$$x = U(t)\cos\omega t - V(t)\sin\omega t \tag{2.31}$$

and substituting it in the equation of motion, we find

$$(\dot{U}) = (\omega - \omega_0)V - \beta U/2 \tag{2.32}$$

$$(\dot{V}) = -(\omega - \omega_0)U - \beta B/2 - F/(2m\omega) \tag{2.33}$$

The total energy of the oscillator in terms of U and V can be calculated to be $E = 1/2m\omega^2(U^2 + V^2)$, approximating the natural and driving frequencies to be equal in magnitude. From the above equations, the rate of change of energy is given by

$$\dot{E} = -\beta E - FV\omega/2 \tag{2.34}$$

Treating the energy of the two-level system similarly, a damping term is introduced to get

$$\dot{\rho_{22}} = -\Gamma\rho_{22} + \Omega v/2 \tag{2.35}$$

where Ω is the driving frequency.

The equations for $\dot{u}$, $\dot{v}$ and $\dot{w}$ become the Optical Bloch equations

$$\dot{u} = \delta v - \Gamma u/2 \tag{2.36}$$

$$\dot{v} = -\delta u + \Omega w - \Gamma v/2 \tag{2.37}$$

$$\dot{w} = -\Omega v - \Gamma(w - 1) \tag{2.38}$$

The steady state solution, i.e. at times longer than the lifetime of the upper level is

$$u = \frac{\Omega\delta}{\delta^2 + \Omega^2/2 + \Gamma^2/4} \tag{2.39}$$

$$v = \frac{\Omega\Gamma/2}{\delta^2 + \Omega^2/2 + \Gamma^2/4} \tag{2.40}$$

$$w = \frac{\delta^2 + \Gamma^2/2}{\delta^2 + \Omega^2/2 + \Gamma^2/4} \tag{2.41}$$

From these equations, the upper state can be calculated to have a steady state population of

$$\rho_{22} = \frac{1-w}{2} = \frac{\Omega^2/4}{\delta^2 + \Omega^2/2 + \Gamma^2/4} \tag{2.42}$$

At a strong driving field ($\Omega \to \infty$), the populations of both the levels tend to become equal, i.e. $w \to 0$ as $\rho_{22} \to 1/2$.

This treatment can be compared to Einstein's treatment of the populations in the two levels. The rate equations for the populations are given by

$$\frac{dN_2}{dt} = N_1 B_{12}\rho(\omega_{12}) - N_2 B_{21}\rho(\omega_{12}) - N_2 A_{21} \tag{2.43}$$

$$\frac{dN_1}{dt} = -\frac{dN_2}{dt} \tag{2.44}$$

where $\rho(\omega_{12})$ is the energy density per unit frequency interval near the atomic frequency, B_{12} and B_{21} are the coefficients for stimulated absorption and emission whereas A_{21} is the coefficient for spontaneous emission.

Considering the atom to be in a region of black body radiation (the energy density of radiation is given by the Planck distribution law) and the system to be in thermal equilibrium (the populations are dependent on the Boltzmann factor), the energy density is given by

$$\rho(\omega_{12}) = \frac{A_{21}}{B_{21}} \frac{1}{(N_1/N_2)(B_{12}/B_{21}) - 1} \tag{2.45}$$

At thermal equilibrium, the relation between the populations of the two states is

$$\frac{N_2}{g_2} = \frac{N_1}{g_1} e^{(-\hbar\omega/k_B T)} \tag{2.46}$$

Using these equations, we get the relationships between the coefficients

$$A_{21} = \frac{\hbar\omega^3}{\pi^2 c^3} B_{21} \tag{2.47}$$

$$B_{12} = \frac{g_2}{g_1} B_{21} \tag{2.48}$$

To compare the two treatments, we start by writing the Rabi frequency in terms of the energy density in frequency intervals,

$$|\Omega|^2 = \left|\frac{eX_{12}E_0(\omega)}{\hbar}\right| = \frac{e^2|X_{12}|^2}{\hbar^2} \frac{2\rho(\omega)d\omega}{\epsilon_0} \tag{2.49}$$

Using this equation and integrating the expression for $c_2(t)$ from the rotating wave approximation over all frequencies in the broadband radiation, we get the transition probability from level 1 to 2 as

$$R_{12} = \frac{|c_2(t)|^2}{t} = \frac{\pi e^2 |X_{12}|^2}{\epsilon_0 \hbar^2} \rho(\omega_0) \tag{2.50}$$

From this, we can write the expression for Einstein's coefficient of absorption as

$$B_{12} = \frac{\pi e^2 |D_{12}|^2}{3\epsilon_0 \hbar^2} \tag{2.51}$$

where $D_{12} = \langle 1|\vec{r}|2\rangle$ and $|X_{12}|^2 = |D_{12}|^2/3$.

With the relation between A_{21} and B_{12}, we find

$$A_{21} = \frac{g_1}{g_2} \frac{4\alpha}{3c^2} \omega^3 |D_{12}|^2 \tag{2.52}$$

where α is the fine structure constant.

When $\Omega \to \infty$ we see that the energy density $\rho(\omega) \to \infty$. If the degeneracies of the two states are equal, the stimulated absorption and emission coefficients are equal. Using the equation for energy density, we see that $N_1/N_2 = 1$, i.e. $\rho_{22} = \rho_{11} = 1/2$. This agrees with the result from the Optical Bloch equations.

2.2 Laser Cooling of atoms

When an atom absorbs a photon, it experiences an impulse of magnitude and direction those of the photon's momentum. A stream of atoms traveling in a light beam constantly absorb and spontaneously emit photons. As the emission is spontaneous, each photon is emitted in a random direction. Thus the impulses received by the emission of photons cancel themselves out over many cycles. If the atoms are traveling in a direction opposite to the photons, the absorption and emission slows down the atoms. As the velocity of the atoms is reduced, the temperature of the atoms given by $K.E = 3/2k_BT$ is also reduced proportionately.

Considering radiation of intensity I, the force on an area A is given by

$$F = \frac{IA}{c} = \frac{P}{c} \tag{2.53}$$

where P is the power of the radiation beam. Atoms subjected to a counter propagating laser beam experience a force

$$F = \frac{-\sigma I}{c}$$

where σ is the absorption cross-section of the atoms.

The magnitude of this scattering force, given in terms of photons absorbed is

$$F = (scattering \;\; rate) \times (photon \;\; momentum) \tag{2.54}$$

The scattering rate is dependent on the population of the upper level of the atoms and is given by $R = \Gamma\rho_{22}$ where Γ is the line-width of the transition between the two levels. Using the expression for the population derived in the previous section,

$$\rho_{22} = \frac{\Gamma}{2}\frac{\Gamma^2/2}{\delta^2 + \Omega^2/2 + \Gamma^2/4} \tag{2.55}$$

where the frequency detuning from resonance should also include the Doppler shift and thus is $\delta = \omega - \omega_0 + kv$. Using the relation between Intensity I and Rabi frequency Ω, $I/I_sat = 2\Omega^2/\Gamma^2$, we can write the force in terms of Intensity as

$$F = \hbar k\frac{\Gamma}{2}\frac{I/I_{sat}}{1 + I/I_{sat} + 4\delta^2/\Gamma^2} \tag{2.56}$$

where I_{sat} is the intensity at which half of the atoms are in the excited state and is called the saturation intensity. Maximum force ($\hbar k\Gamma/2$) is experienced when I is much greater than I_{sat}. Another explanation for this is that the atoms spend half their time in the excited state and the rate of absorption

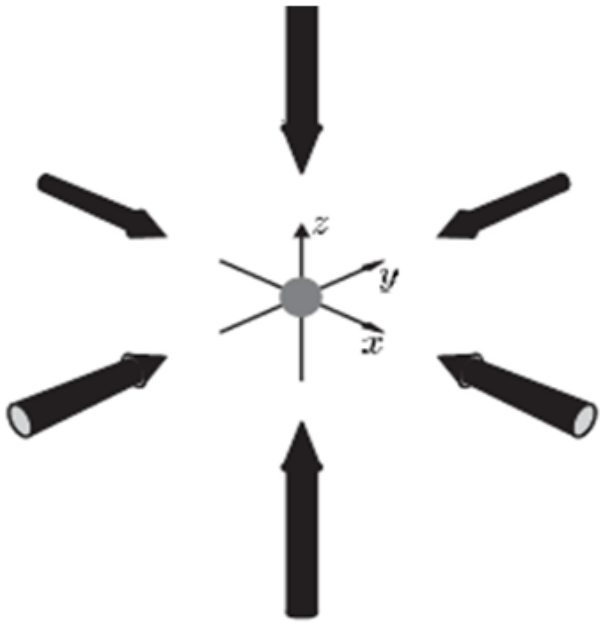

Figure 2.1: Configuration of Optical Molasses technique

of photons is $1/2\tau$ where τ is the lifetime of the excited state. The recoil velocity experienced by the atom of mass M is $v_r = \hbar k/M$. Therefore, the maximum acceleration is

$$a_{max} = \frac{v_r}{2\tau} = \frac{\hbar k \Gamma}{2M} \tag{2.57}$$

2.2.1 Optical Molasses

A laser beam slows down atoms moving only in the direction opposite it, or rather it reduces only the component of velocity that is opposite to it. But atoms in a gas move in all three directions. Reducing the speed of the atoms requires laser cooling in all three directions. This is implemented by creating three orthogonal standing waves. The figure shown represents the configuration.

Because of the Doppler effect, a moving atom 'sees' an increase in the frequency of the laser beam propagating in the direction opposite to it. Using red detuned light for all the beams, we ensure that the atoms mostly absorb the photons traveling opposite to them. This reduces the velocity of the

atoms in all three directions.

The force experienced by the atoms due to the two counter-propagating beams along one axis, say the z-axis, can be expressed as [24]

$$F_{molasses} = F_{scatt}(\omega - \omega_0 - kv) - F_{scatt}(\omega - \omega_0 + kv) \tag{2.58}$$

$$= F_{scatt}(\omega - \omega_0) - kv\frac{\partial F}{\partial \omega} - [F_{scatt}(\omega - \omega_0) + kv\frac{\partial F}{\partial \omega}] \tag{2.59}$$

$$= -2\frac{\partial F}{\partial \omega}kv \tag{2.60}$$

$$= 4\hbar k^2 \frac{I}{I_{sat}} \frac{-2\partial/\Gamma}{[1 + (2\partial/\Gamma)^2]^2} \tag{2.61}$$

The constant $2k\frac{\partial F}{\partial \omega}$ is denoted by α, giving the damping force $F_{molasses} = -\alpha v$.

The kinetic energy of the atoms along the z-axis changes as

$$\frac{d}{dt}\left(\frac{1}{2}Mv_z^2\right) = Mv_z\frac{dv_z}{dt} = v_z F_{molasses} = -2k\frac{\partial F}{\partial \omega}v_z^2 \tag{2.62}$$

Similar equations apply to the other axes. The total kinetic energy $E = \frac{1}{2}M(v_x^2 + v_y^2 + v_z^2)$ decreases where the three orthogonal beams intersect.

$$\frac{dE}{dt} = -\frac{2\alpha}{M}E = -\frac{E}{\tau_{damp}} \tag{2.63}$$

Usually, the damping time τ_{damp} is a few microseconds.

2.2.2 The Magneto-Optical Trap

The optical molasses technique with a quadrupole magnetic field can be used to trap atoms. Two coils with currents in the opposite directions produce the required magnetic field. The laser beams should have circular polarizations, with each pair of counter propagating beams having polarizations opposite to each other. The schematic of the trap is shown in the figure.

The magnetic fields from the two coils cancel each other at the centre in between the coils. There is a uniform gradient of field such that the Zeeman effect is linear. When the atoms move from the centre towards one side, the magnetic field there causes its levels to split in such a way that absorption of photons from the laser beam travelling opposite to the atom becomes favourable. the laser beams are red detuned. As the atoms tend to absorb more photons from the beam traveling opposite to it than from that traveling along it, it experiences a force damping its motion (as explained in

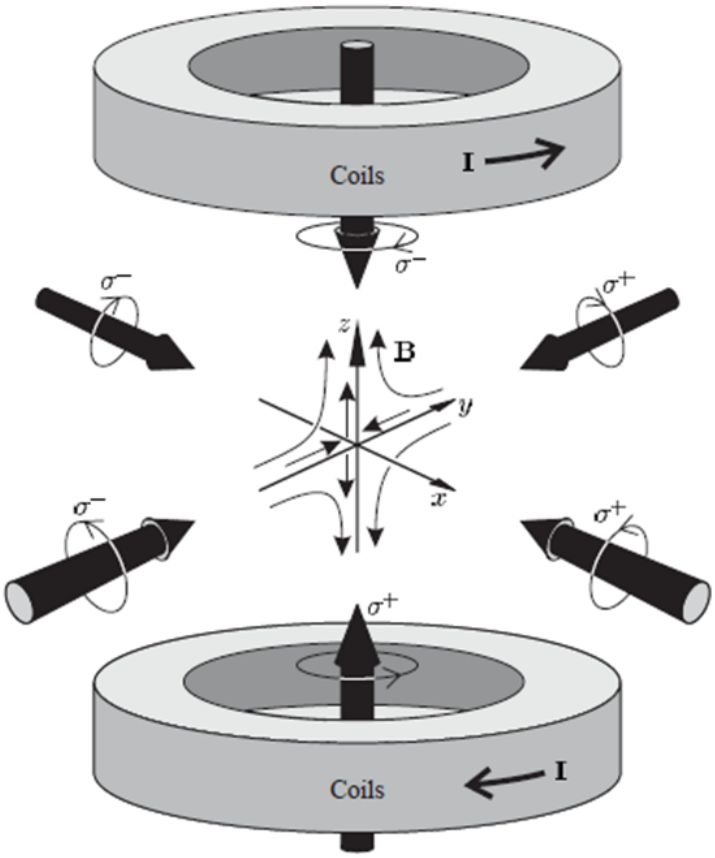

Figure 2.2: The Magneto-Optic Trap

the optical molasses section). Similarly, the atoms experience a force from all directions pushing them back towards the centre.

Considering that the atom moves in such a way that the σ^+ transition becomes favourable, the force that the atom experiences is given by the expression [24]

$$F_{MOT} = F^{\sigma^+}_{scatt}(\omega - kv - (\omega_0 + \beta z)) - F^{\sigma^-}_{scatt}(\omega + kv - (\omega_0 - \beta z)) \quad (2.64)$$

$$= -2\frac{\partial F}{\partial \omega} kv + 2\frac{\partial F}{\partial \omega_0}\beta z \quad (2.65)$$

The terms $\omega_0 + \beta z$ and $\omega_0 - \beta z$ are the resonant absorption frequencies for the σ^+ and the σ^- transitions respectively. The Zeeman shift βz at displacement z is

$$\beta z = \frac{g\mu_B}{\hbar}\frac{dB}{dz} z \quad (2.66)$$

As the frequency detuning $\delta = \omega - \omega_0$ is kept constant,

$$\frac{\partial F}{\partial \omega_0} = -\frac{\partial F}{\partial \omega} \tag{2.67}$$

Therefore,

$$F_{MOT} = -2\frac{\partial F}{\partial \omega}(kv + \beta z) \tag{2.68}$$

$$= -\alpha v - \frac{\alpha\beta}{k} z \tag{2.69}$$

The restoring force has a spring constant $\alpha\beta/k$. The atoms are slowed down in the region of intersection of the orthogonal beams and are pushed towards the centre of the trap as the force is also position dependent. Thus atoms are loaded in the centre of the trap.

2.2.3 Zeeman Slower

Only the atoms with velocities below a certain value can get captured in the MOT. This capture velocity is dependent on the detuning of the laser beams and the gradient of the magnetic field and is typically a few tens of m/s. Atoms with higher velocities do not spend enough time in the laser beams to slow down sufficiently. The initial velocity of the atoms is decided by the temperature and pressure in the oven to get the required initial flux of atoms. A Zeeman Slower is used to slow down the atoms from the initial velocities of a few hundred m/s to a few tens m/s.

As the atoms slow down, the Doppler shift (kv) also reduces proportionately. In the equation for the scattering force, the detuning δ took into account the Doppler shift also. This implies that as the Doppler shift reduces, the laser frequency is no longer in tune with the atomic frequency and the absorption of photons reduces. One way to account for this change in the Doppler shift is incorporated in the design for the Zeeman Slower. The atoms slow down over a certain length. A spatially varying magnetic field is applied over this length such that the Zeeman effect moves the atomic levels to compensate for the varying Doppler shift. As the transition frequency changes, the laser frequency required for the absorption to take place remains constant. The schematic diagram for a Zeeman Slower, including the oven and the UHV chamber is shown.

The magnetic field profile should satisfy the condition [24]

$$\omega_0 + \frac{\mu_B B(z)}{\hbar} = \omega + kv \tag{2.70}$$

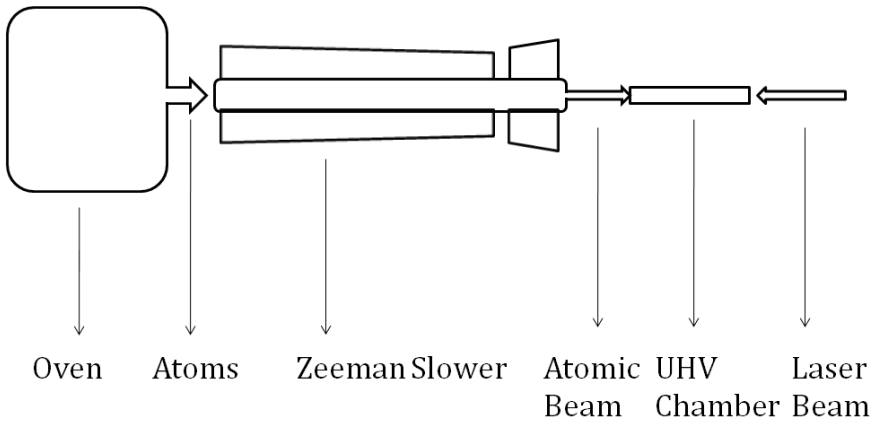

Figure 2.3: Schematic of Zeeman slower

where z is the distance from the beginning of the slower to that point, v is the speed of the atoms, μ_B is the Bohr magneton, k is the magnitude of the wave vector, ω_0 is the atomic frequency and ω is the laser frequency.

The velocity of the atoms as a function of z is given by

$$v = v_0(1 - \frac{z}{L_0})^{1/2} \tag{2.71}$$

where v_0 is the highest initial velocity from which atoms can slow down which determines the length of the Slower.

From the above equations, the magnetic field profile can be calculated to be

$$B(z) = B_0(1 - \frac{z}{L_0})^{1/2} + B_{bias} \tag{2.72}$$

where $B_0 = \hbar k v_0/\mu_B$ and $B_{bias} = (\omega - \omega_0)\hbar/\mu_B$.

Atoms with velocities higher than the v_0 taken are not affected significantly by the laser beam. The atoms with velocities lesser than v_0 move unimpeded until they reach the point where the magnetic field is $B = \hbar k v/\mu_B$, from where they decelerate continuously with the atomic frequency being in resonance with the laser frequency.

2.3 2D-MOT to 3D-MOT

Loading atoms into a 3D-MOT requires a continuous beam of cold atoms with a small divergence. Apart from chirped slowers and loading directly from vapour pressure (significant mostly for heavier atoms), Zeeman Slowers are also used as a continuous source. A Zeeman slower decelerates an atomic beam in one direction, but this gives rise to a high divergence beam. By implementing a technique in which one of the beams in a 3D-MOT is dark, Lu et.al. [25] have produced a continuous collimated beam that travels in the direction in which there is the imbalance of radiation pressure. Another way to load atoms is to use a double MOT system, in which the first MOT produces an atomic beam with the required specifications for loading in the second MOT. The second MOT is the usual 3D-MOT described in the previous section, whereas the first MOT is 2 dimensional. The four orthogonal laser beams that make up a 2D MOT are perpendicular to the axis of propagation of the atomic beam. Initially, Riis et.al [26] have used this technique to extract very slow atoms out of an already cooled beam. Now this procedure can be implemented to produce a slow atomic beam directly from vapour pressure.

There are two kinds of 2D-MOT systems that can produce the required flux for a 3D-MOT system. A Pure 2D-MOT system has only four beams of laser on the axes perpendicular to the propagation axis. This can produce a flux that is of the order of 10^{10}, comparable to a Zeeman Slower output flux. As there are no laser beams along the axis of propagation, there will not be any background noise in the 3D MOT chamber due to the laser beams in the 2D MOT chamber. On the other hand, a $2D^{+}$-MOT (realized by Dieckmann et al. [27]), has an additional laser beam copropagating with the atoms and pushing them towards the 3D-MOT system. This can produce a flux of the order of 10^{9} atoms/s. The advantage of this system is that atoms can be loaded with smaller powers of cooling lasers, as even the lowest velocity atoms are pushed towards the 3D MOT loading area.

2.3.1 The Pure 2D-MOT system

The vapour cell and the Ultra-high Vacuum chamber are connected by a differential pumping tube. The UHV chamber needs a pressure of about 10^{-10} Torr for the 3D MOT system, whereas the vapour call can have a pressure of about 10^{-8} to 10^{-7} Torr for the 2D MOT. The intersection of the four orthogonal counter propagating laser beams makes up the cooling volume. Also, there are four coils which produce a two-dimensional magnetic field whose line of zero field is along the centre axis (the longitudinal axis) of

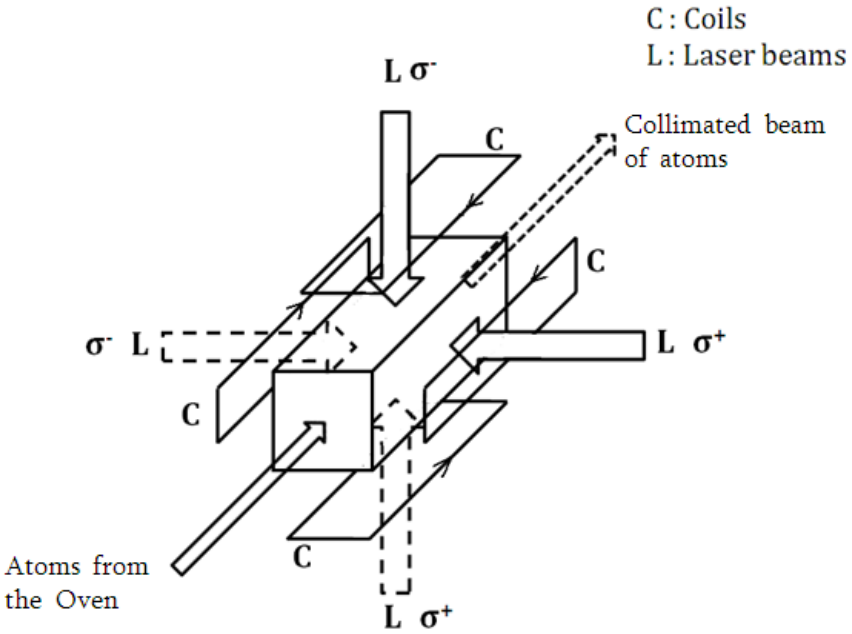

Figure 2.4: The 2D MOT Chamber

the cell and the pumping tube. The cooling volume also encloses this axis. It should be ensured that this volume extends to the mouth of the pumping tube.

The schematic of the 2D MOT chamber is shown.

The atoms' velocity along this axis (the longitudinal axis) is not reduced. The atoms are slowed down only in the two transverse axes. Therefore, the atoms are pushed towards the centre axis following the trajectory of a damped harmonic oscillator in two dimensions while moving along the longitudinal axis without impediment. We define a new velocity called the radial velocity which is rms value of the two transverse velocities. The output of the cooling volume is a collimated atomic beam moving either towards the entrance of the tube or the back wall of the cell. We consider only the atoms moving forward as the atoms moving backward collide off the wall.

The atoms in the collimated beam that enter the pumping tube will have satisfied the following three conditions.

1. The initial radial velocity component has to be lesser than the radial capture velocity of the 2D-MOT. Or else, the atoms will pass through the cooling volume and not get collimated into the output beam.

2. The radial velocity should be sufficiently reduced so that the atoms in the beam reach the UHV chamber. For this, the longitudinal velocity should be small enough so that the atoms have enough time to interact with the laser beams. If not, the atoms will hit the walls of the pumping tube and might not reach the UHV chamber.

3. The cooling process of the atoms should not suffer because of collisions. The mean free path of the atoms in the vapour cell should be of the order of the length of the cooling volume.

The process of cooling in this system can be described in two regimes: the collisionless regime and the collisions regime [28].

Collisionless Regime

In this regime, the mean free path of the atoms in the vapour cell should be greater than the length of the cell. As there are no collisions between atoms, the contribution to the output flux is decided only by the initial conditions of the atoms. Atoms possessing very low radial velocities and very high longitudinal velocities can still pass through the aperture and contribute to the thermal background in the UHV chamber. All the atoms that start on the sides of the cell can enter the aperture only if they are cooled sufficiently.

The total flux is dependent on the following factors.

1. The time which atoms spend in the cooling volume which is dependent on their longitudinal velocity and position at which they entered they volume. This implies that the radial capture velocity depends on z and v_z. Also, as the cooling time is finite, the percentage of atoms with smaller v_z increases.

2. The longer the cooling length, the more atoms with higher initial radial velocities can enter the tube.

3. The higher the laser intensity, the more efficient radial cooling is, until I_{sat} dominates.

4. The length of the 2D MOT affects the radial capture velocity. The longer the length, the greater the velocities of atoms which can go through the aperture. This implies that the mean longitudinal velocity also becomes higher (as a fraction of the total velocity). In an infinitely long 2D MOT, the longitudinal velocity distribution will be that of a normal thermal distribution.

5. As pressure increases, the number of atoms which can be trapped increases (with the total number of atoms) and so does the flux too.

Collisions Regime

The atoms in the cooling can thermalize due to collisions. This increases the percentage of thermal atoms in the output flux. As described previously, the flux increases with the MOT length. But this increase is controlled /limited by the background gas collisions and light assisted collisions of excited atoms with the background gas.

The mean number of collisions and the mean time of interaction with laser radiation are given by

$$\Gamma = n\sigma v \tag{2.73}$$

$$\tau = \frac{< z >}{v_z} \tag{2.74}$$

where σ is the collision cross section and n is the number density in the cell.

As the MOT length increases, the mean number of collisions increases, therefore more atoms could get lost. Combined with the dependence of MOT length explained previously, we see that the output flux has to reach a maximum at some length and stay saturated. As the atoms with smaller longitudinal velocities spend more time in the cooling volume, the probability of loss due to collisions is higher for them. Therefore, the average velocity of the output flux increases.

An increasing pressure in the cell gives rise to more collisions in the cooling volume thereby decreasing the effective length of the MOT. The ideal pressure at which the MOT should be operated is when the mean free path of the atoms is of the same order as of the dimensions of the cooling volume. If the pressure is too high, more atoms absorb photons and this decreases the average cooling of one atom.

2.3.2 Theoretical description

A rate model is used to describe the output flux of the 2D MOT system theoretically. A model for the longitudinal velocity distribution of the output flux can be derived [28].

We start with defining a function Φ to describe the integrated flux per velocity interval $[v_z, v_z + dv_z]$

$$\hat{\Phi}(n, v_z) = \frac{\int_0^L R(n, v_z, z) e^{-\Gamma_{coll}(n) z / v_z} dz}{1 + \frac{\Gamma_{trap}(n)}{\Gamma_{out}}} \tag{2.75}$$

where Γ_{trap} is the loss rate out of the cloud and Γ_{out} is the outcoupling rate from the trapping region, L is the length of the cooling volume and R is loading rate of the atoms into the MOT. The exponential loss term containing the collision rate describes loss due to light assisted collisions between atoms and background gas. The total output flux is the integral of $\hat{\Phi}$ over all positive v_z.

$$\Phi = \int_0^\infty \hat{\Phi}(n, v_z) dv_z \tag{2.76}$$

The loading rate R for the 2D MOT is derived by defining the rate per longitudinal velocity interval $[v_z, v_z + dv_z]$.

$$R(n, v_z, z) = nd\frac{16\sqrt{\pi}}{u^3} exp(\frac{-v_z^2}{u^2}) \int_0^{v_c(v_z,z)} v_r^2 exp(\frac{-v_r^2}{u_2}) dv_r \tag{2.77}$$

where d is the length of the cooling volume, u the most probable velocity of the thermal distribution (Maxwell-Boltzmann distribution) and T the temperature of the vapour. v_r is the radial velocity and v_c the capture velocity dependent on v_z and z as discussed above. For each v_z the rate is loaded with the fraction of the Boltzmann distribution that can be cooled to enter the flux.

v_c is defined by the following expression

$$v_c(v_z, z) = \frac{v_{c0}}{1 + v_z/v_{cr}} \tag{2.78}$$

This satisfies the two conditions on the capture velocity in the limiting cases as explained below. v_{cr} is the critical velocity below which the cooling time is independent of v_z. This happens at the lower limit of v_z. Here, the capture velocity is equal to a constant v_{c0}. Above the critical velocity (at higher v_z) the cooling time is dependent on the longitudinal velocity and the capture velocity falls off as $1/v_z$. v_{cr} is calculated by equating the mean longitudinal flight time and the radial cooling time. This gives the following equations.

$$\frac{L}{2v_{cr}} = \frac{d}{v_{c0}} v_{cr} = \frac{Lv_{c0}}{2d} \tag{2.79}$$

Finally, we write the expression for the output flux of each velocity interval $[v_z, v_z + dv_z]$ using all the equations above

$$\hat{\Phi}(n, v_z) = \frac{nd}{1 + \frac{\Gamma_{trap}(n)}{\Gamma_{out}}} \frac{16\sqrt{\pi}}{u^3} \frac{v_z}{\Gamma_{coll}} exp\left(\frac{-v_z^2}{u^2}\right) \left(1 - \left(-\Gamma_{coll}\frac{L}{v_z}\right)\right) \int_0^{v_c} exp\left(\frac{-v_r^2}{u^2}\right) \tag{2.80}$$

Integrating this expression over v_z will give us the total output flux.

2.4 Oven Collimation system

The temperature of the oven is decided based on the pressure needed for the desired flux. A collimation system in between the oven and the first stage of laser cooling (Zeeman Slower or a 2D MOT) will ensure that most of the atoms that enter the stage are cooled down and do not contribute to the thermal background in the 3D MOT stage.

The atoms leave the oven by a process called effusion. If the hole in the oven chamber is much smaller than the mean free path of the atoms at that temperature and pressure, then the only atoms leaving the oven from that hole would be the atoms that would have hit that area. As the mean free path is much greater than the dimensions of the hole, no collisions are expected to happen near the mouth of the exit. This implies that the other atoms still present in the chamber are negligibly affected by the exit of these atoms. This regime is called the molecular flow regime. On the other hand, if the dimensions of the hole are comparable to the mean free path, the atoms undergo frequent collisions with each other near the hole. As a few atoms leave the chamber through the hole, the other atoms present near the hole will experience a deficit of collisions from that direction thereby acquiring a drift velocity towards the hole, and eventually out of it. Therefore, the number of atoms that leave the chamber is more than the number of atoms that would have struck the area of the hole had it been closed. This process is called the hydrodynamic flow. The regimes are characterized by the Knudsen's number $\mathrm{Kn} = \frac{\lambda}{d}$ where λ is the mean free path of the atoms and d is the dimension of the hole. The hydrodynamic flow regime has $\mathrm{Kn} < 0.01$ and the molecular flow regime has $\mathrm{Kn} > 1$.

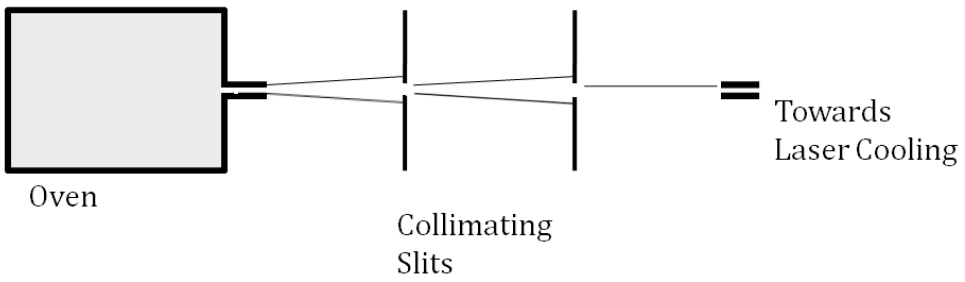

Figure 2.5: Oven Collimating System

At the temperature and pressure that an oven chamber is usually at, the mean free path of the atoms will be a few meters. In this regime, the flow of atoms out of the oven is effusion. A tube connects the oven and the vacuum chamber next to it. The hole in the oven chamber is attached to the mouth of the tube. The diameter of the tube (d) is usually 8 mm to 1 cm and the length of the tube (L) is about 10 cm to 15 cm. The divergence of the beam coming out of this tube is about 0.067 rad. One or two more obstructs can be placed in the path of the atomic beam coming out of this tube. The divergence and the flux of the final beam will depend on the sizes of the holes in these two obstructs.

The flux of atoms in the velocity range [v,v+dv] emerging from the hole of area A into a solid angle range $d\Omega$ is given by the equations [29]

$$A\Phi(\vec{v})d^3\vec{v} \propto A[f(v)v\cos\theta](v^2 dv d\Omega) \tag{2.81}$$

$$\propto f(v)v^3 dv d\Omega \tag{2.82}$$

$$\propto exp\left(-\frac{mv^2}{2kT}\right)v^3 dv d\Omega \tag{2.83}$$

where θ is the angle of divergence. This expression is proportional to v^3 whereas the Maxwell velocity distribution is proportional to v^2.

2.5 Strontium atomic system

Strontium is an alkaline-earth metal with atomic number 38. Its relative atomic mass is 87.62 and its vapour pressure is 1.39×10^{-9} Torr at 500-600 Kelvin. Its electronic configuration (two electrons in its valence shell) gives rise to properties unique to alkaline-earth atoms that can be used for research in many areas. It is found in nature as Celestite ($SrSO_4$) and Strontianite ($SrCO_3$). It has four naturally occurring isotopes- ^{84}Sr, ^{86}Sr, ^{87}Sr and ^{88}Sr whose relative abundances are given below [30].

Isotope	Abundance
^{84}Sr	0.56
^{86}Sr	9.86
^{87}Sr	7
^{88}Sr	82.58

Three of the isotopes ^{84}Sr, ^{86}Sr and ^{88}Sr are Bosonic (nuclear spin 0) and one isotope ^{87}Sr is Fermionic with nuclear spin 9/2. These isotopes in different combinations have a wide range of scattering lengths [31]

Combination	Length (a_0)
88-88	-2.01
87-87	96.7
86-86	799.5
84-84	122.8
88-87	54.8
88-86	97.9
88-84	1656.8
87-86	161.1
87-84	-57.7
86-84	31.5

2.5.1 Level Diagram

The level diagram of Strontium-87 is as shown.

The $^1S_0 - ^1P_1$ and $^1S_0 - ^3P_1$ transitions are used for laser cooling whereas

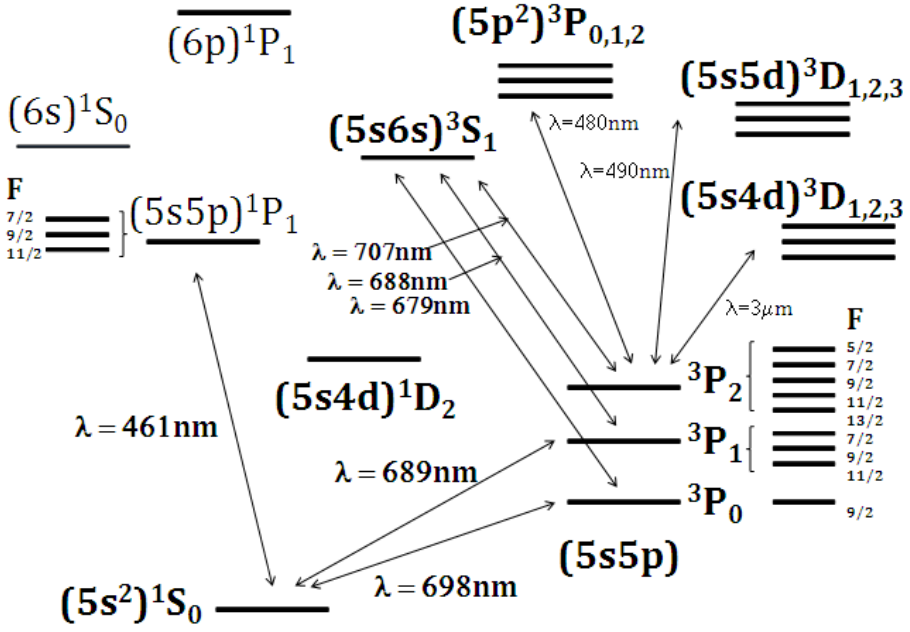

Figure 2.6: Level Diagram of Strontium

the ${}^1S_0 - {}^3P_0$ is used as the clock transition (this is the transition probed in optical clock experiments). The hyperfine splitting of the levels relevant for laser cooling is shown. The life-times of the levels are given in the table below.

Level	Life-time
(5s5p) ${}^1P_1$	5.22ns
(5s5p) ${}^3P_0$	150s
(5s5p) ${}^3P_1$	21.4μs
(5s6s) ${}^3S_1$	11.8ns
($5p^2$) ${}^3P_{0,1,2}$	7.9ns
(5s4d) ${}^3D_{1,2,3}$	2.9 μs
(5s5d) ${}^3D_{1,2,3}$	16ns

2.5.2 Laser cooling

The ${}^1S_0 - {}^1P_1$ transition with a wavelength of 461 nm and a linewidth of 32 MHz is very good for laser cooling. It can achieve high cooling rates as it has a broad line-width. Laser cooling on this transition can reduce the

temperature of the atoms to a few hundred microkelvins.

The narrow inter-combination transition $^1S_0 - ^3P_0$ with a wavelength of 689 nm and a line-width of 7.6 KHz has a Doppler limit which is three orders lesser than the other transitions. Laser cooling on this transition can reduce the temperature to a few microkelvins or even a few hundred nanokelvins.

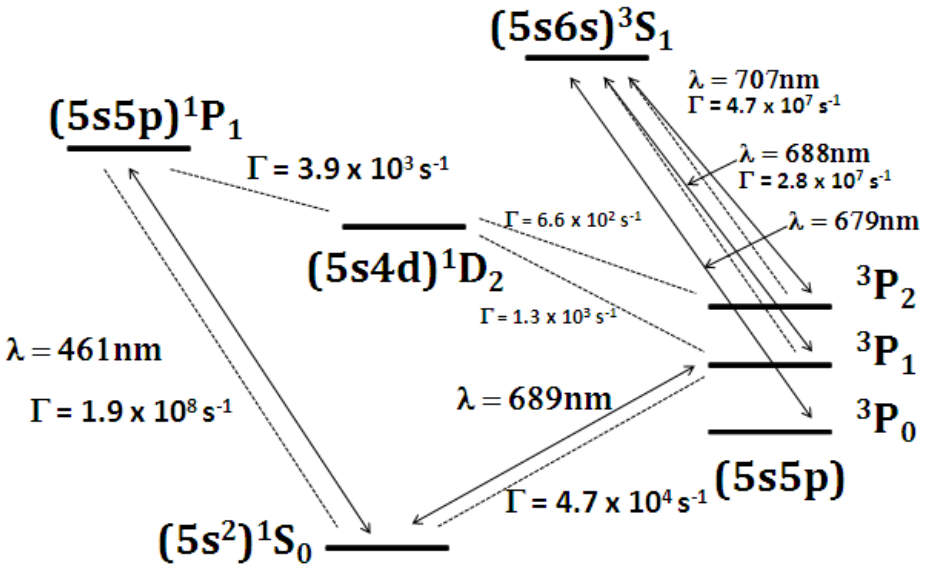

Figure 2.7: Transitions used in laser cooling

Atoms in the $^1P_1$ state branch out to the $^1D_2$ state with a ratio of about 1 in 50,000. These atoms decay to $^3P_1$ and $^3P_2$ states. The atoms in the $^3P_1$ state decay back to the ground state thereby closing the cycle. But the atoms in the $^3P_2$ can't decay to the ground state. They have to be pumped into the $^3S_1$ state with a laser beam of wavelength 707.2 nm. These atoms now decay either to the $^3P_0$ or the $^3P_2$ state. Atoms from the former state can decay naturally to the ground state and those in the latter state are pumped into the $^3S_1$ state again and eventually reach the ground state. Thus it is ensured that the atoms are continuously cooled by the 461 nm laser beam without significant losses.

2.5.3 Zeeman Effect in the Slower

The perturbation of the hyperfine levels due to the Zeeman effect in the presence of a magnetic field is used in the design of a Zeeman slower to

keep the atomic transition in resonance with the frequency of the laser. The energy of the different levels changes as the m_F and g_F values of the levels.

The g_F values are calculated using the following two equations.

$$g_J = 1 + \frac{J(J+1) + S(S+1) - L(L+1)}{2J(J+1)} \tag{2.84}$$

$$g_F = g_J \times \frac{F(F+1) + J(J+1) - I(I+1)}{2F(F+1)} \tag{2.85}$$

The F and g_F values for the relevant levels are given as follows.

State	F	g_F
$^1S_0$	9/2	0
$^1P_1$	7/2	-2/9
$^1P_1$	9/2	4/99
$^1P_1$	11/2	2/11

The transition from the level $^1S_0$, F = 9/2, m_F = 9/2 to the level $^1P_1$, F = 11/2, m_F = 2/11 is chosen as it satisfies the condition $\Delta m = \pm 1$, it decreases the atomic frequency and it gives the least range of the magnetic field required.

g_F of the $^1S_0$ state is taken to be zero as it does not have any electric moment and the effects of the nuclear magnetic moment are about three orders lesser than those of the electric moment (μ_B is 1.44 MHz/G whereas μ_I is 200 Hz/G) and hence negligible. In the diagram given, the effects of a magnetic field upto 500 G are shown for the $^1S_0$ F= 9/2 and $^1P_1$ F = 11/2 states. The excited state has a sensitivity proportional to μ_B whereas the ground state has a sensitivity proportional to μ_I. The Lande-g factor for the ground state is taken as g_I given by the equation

$$g_I = \frac{\mu_I(1-\sigma_d)}{\mu_0|I|} = 0.868 \tag{2.86}$$

The change in the values of energy of different levels with magnetic field is given by the Breit-Rabi formula

$$E(F = I \pm 1/2, m_F) = -\frac{E_{hf}}{2(2I+1)} \pm 1/2 \sqrt{E_{hf}^2 + \frac{4m_f g_J \mu_B B E_{hf}}{2I+1} + (g_J \mu_B B)^2} \tag{2.87}$$

At higher values of the magnetic field, the quadratic values are significant and cannot be ignored. But at lower values, the effect can be approximated by a linear equation

$$\Delta E = -m_F g_F \mu_B B \tag{2.88}$$

The diagram of the Zeeman splitting of the levels $^1S_0$ and $^1P_1$ upto a magnetic field of 500 G is shown. The linear approximation holds in this regime and we only need a magnitude of around 300 G in the Zeeman Slower.

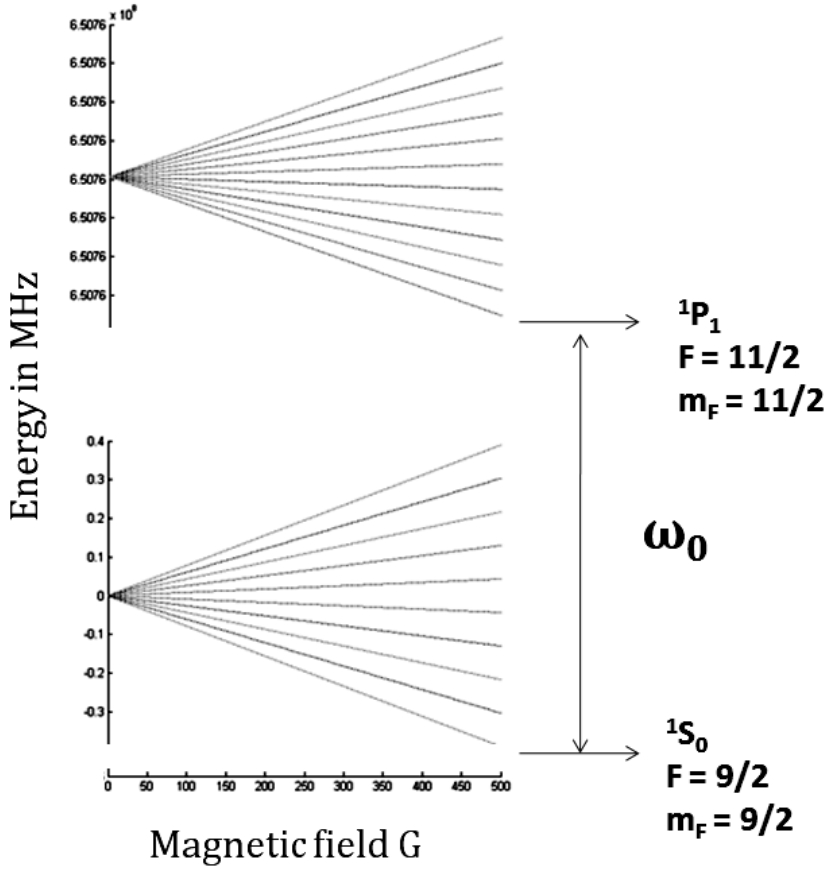

Figure 2.8: Zeeman Effect on the $^1S_0$ F$= 9/2$ and $^1P_1$ F $= 11/2$ states

Chapter 3

Experiment

3.1 Design of the Zeeman Slower

The length over which the atoms slow down depends on the deceleration they experience. A few quantities should be calculated before the slower is designed.

1. The recoil velocity of a Strontium atom given by $\hbar k/M$ is 0.98 cm/s.
2. The maximum deceleration of the atoms when the $Intensity \gg I_{sat}$ given by $v_r/2\tau$ is 0.98×10^8 cm/s^2, where τ the lifetime of the excited state is 5.22 ns.
3. When the temperature of the atoms is 900 K, the pressure in the oven is 3.5×10^{-8} Torr and the average velocity given by $1/2mv^2 = 3/2\ k_BT$ is 423 m/s.
4. The minimum length required given by $v^2/2a_{max}$ is 10.77 cm, where v is taken to be 450 m/s.
5. The minimum time required for the process is $\bar{v}/a_{max} = 478.7$ ms.
6. The number of photons that are absorbed on an average by one atoms is $v/v_{rec} = 45.92 \times 10^3$.

The damping is proportional to the slope of the force curve at $v = 0$. The slowing process is unstable when the force is maximum, but stable when the force is multiplied by a factor of ϵ around 0.75. Also, the force is maximum only when $I \gg I_{sat}$. This is not very feasible experimentally as I_{sat} for Strontium is 40.7 mW/cm^2. We consider a lesser I for the experiment and this reduces the force even more.

Taking into account the above two factors, we modify the equation for the scattering force into

$$F = \epsilon \frac{\hbar k \Gamma}{2} \frac{I/I_{sat}}{1 + I/I_{sat} + 4[\delta_0 + kv - \mu B(z)/\hbar]^2/\Gamma^2} \tag{3.1}$$

As shown in the previous chapter, the magnetic field profile is taken to satisfy the equation

$$B(z) = \frac{\hbar}{\mu_B}[kv(z) + \delta_0] \tag{3.2}$$

$$= B_0 kv(z) + B_{bias} \tag{3.3}$$

and the velocity of the atoms changes as

$$v(z) = v_0 \left(1 - \frac{z}{L}\right)^2 \tag{3.4}$$

where v_0 is the initial average velocity and L is the distance over which the atoms slow down given by $v_0^2/2a$.

The values of ϵ and I are taken to be 0.7 and 30 mW/cm^2 respectively. The deceleration of the atoms can be found out by substituting these values in the equation

$$a = -\frac{\epsilon}{M} \frac{\hbar k \Gamma}{2} \frac{I/I_{sat}}{1 + I/I_{sat}} \tag{3.5}$$

L is calculated for this deceleration and using the above equations, the theoretical magnetic field profile can be found out. The value of B_0 is calculated using

$$B_0 = \frac{\hbar k v_0}{\mu_B (g_e m_e - g_g m_g)} \tag{3.6}$$

where m_e and m_g are the m_F values of the excited and ground states, g_e and g_g are the Lande-g factors of the respective levels. The transition is taken to be from the $^1S_0$ F $= 9/2$ $m_F = 9/2$ state to the $^1P_1$ F $= 11/2$ $m_F = 11/2$ state. The Lande-g factor of the excited state is calculated to be $2/11$ and that of the ground state is negligible compared to the value of the excited state. Taking these values, the value of B_0 comes out to be 687.2 G. To minimize power consumption, we take a bias field $B_{bias} = -350$ G. The detuning of the laser is given by $B_{bias}\mu_B/\hbar$ which is calculated to be 3.12 GHz red detuned from the atomic resonance.

The graph below shows the magnetic field profile for the values given.

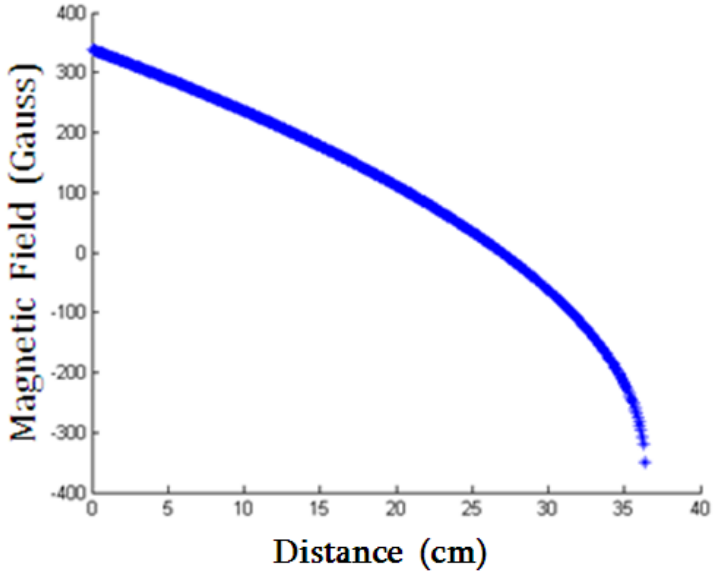

Figure 3.1: Required Magnetic field calculated theoretically

3.2 Simulation of the Magnetic field

The required magnetic field can be created using a solenoid coil. The range of the field is about 700 G. Producing a field of this magnitude would require a lot of power. Therefore, as given in the previous section, we assume a bias field of about half the magnitude of the required field. The solenoid will now have two sections creating magnetic fields of equal magnitude but opposite signs. This would require much lesser power than the other alternative.

The solenoid is designed by wrapping layers of coils around a tube, with decreasing number of coils in the higher layers. A programme in MATLAB is used to simulate the magnetic field along the axis of the solenoid. With this programme, the number of layers and the number of coils in each layer are optimized. The magnitude of the current through the two sections of the coils was decided by simulating the magnetic field for different values of currents and then optimizing the fit of the simulation to the theoretical field profile. The power consumed by the coils is also another factor that was considered before finalizing the values of the currents.

A Zeeman Slower tube of radius 2.1 cm is used. The required length of the Slower is 36.2 cm. The outer diameter of the coil used for the windings is 3.8 mm. An extra ten coils were wound on the negative section towards the outer end as the slope in that region is very steep and these extra windings in each layer brought the minimum of the field in that area as low as possible. This increased the length of the Zeeman Slower to approximately 40 cm.

The simulated field along with the theoretical field is given in the diagram below.

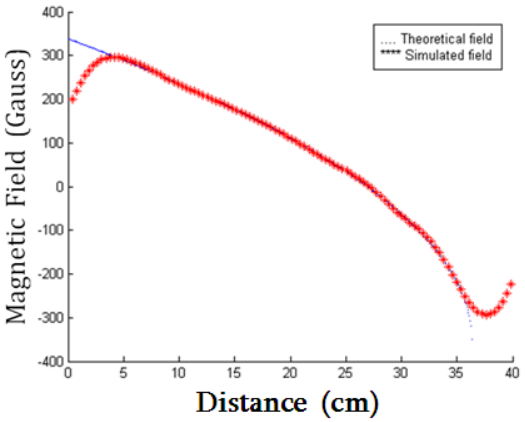

Figure 3.2: Simulated field profile

3.3 Measuring the magnetic field

A Zeeman Slower tube with a radius of 2.1 cm was used. The required length of the Slower is 40 cm. Coils were wound on this tube according to the simulation. The outer diameter of these coils was 3.8 mm and the conduction area 2.5 sq.mm. The positive section had nine layers and needed approximately 60 m of coil, whereas the negative section had ten layers and needed 25 m of coil. According to the simulation, the positive section coils needed to carry 15 A current and the negative section coils 20 A.

The array of the number of coils in the positive section is [73 57 50 40 28 18 13 11 8] and that of the negative section starting from the outer end is [32 16 14 12 12 10 8 6 4 3]. A small region in the positive section near the 25 cm mark needed three extra coils carrying the negative current to get a better match to the theoretical profile. A few meters were left on either side of the two sections for rewinding if any modifications seemed required after the testing. The figure shows the windings of coils.

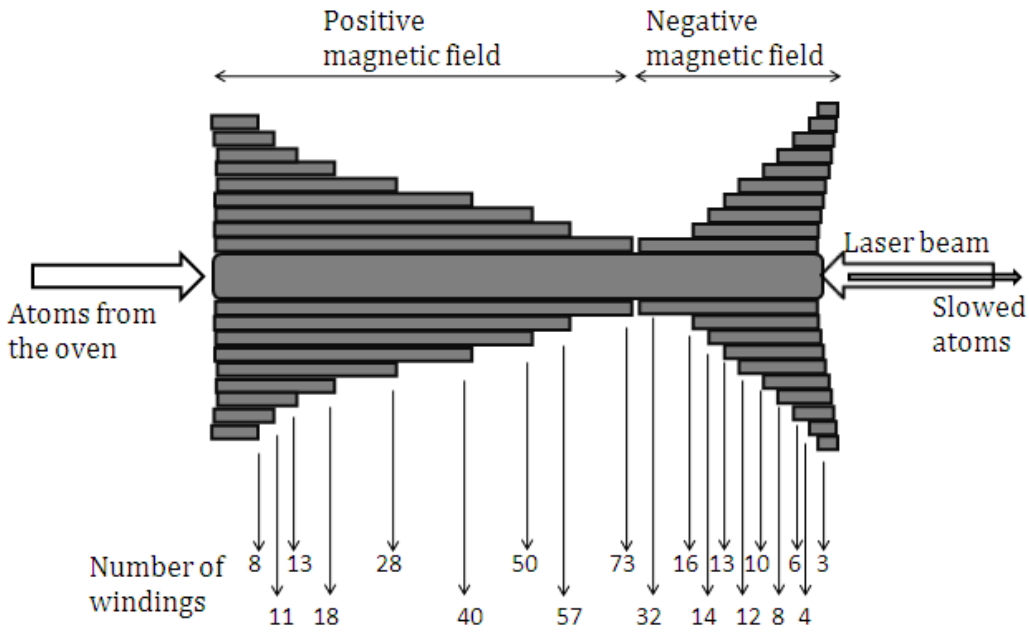

Figure 3.3: The distribution of coils on the Zeeman Slower

The positive current carrying coil was connected to a power supply with 8.2 V across it and the negative current coil to a power supply with voltage 6.4 V. The extra coil on either section was placed as far away from the tube as possible. The magnetic field inside the solenoid was measured using a Gaussmeter probe. The probe was mounted in a copper tube with a measurement tape on it and slid into the slower. The value of the magnetic field was noted every 0.5 cm.

Chapter 4

Results

4.1 Measured Magnetic field profile

The magnetic field profile measured in the solenoid in the experiment is given in the figure below along with the simulated profile.

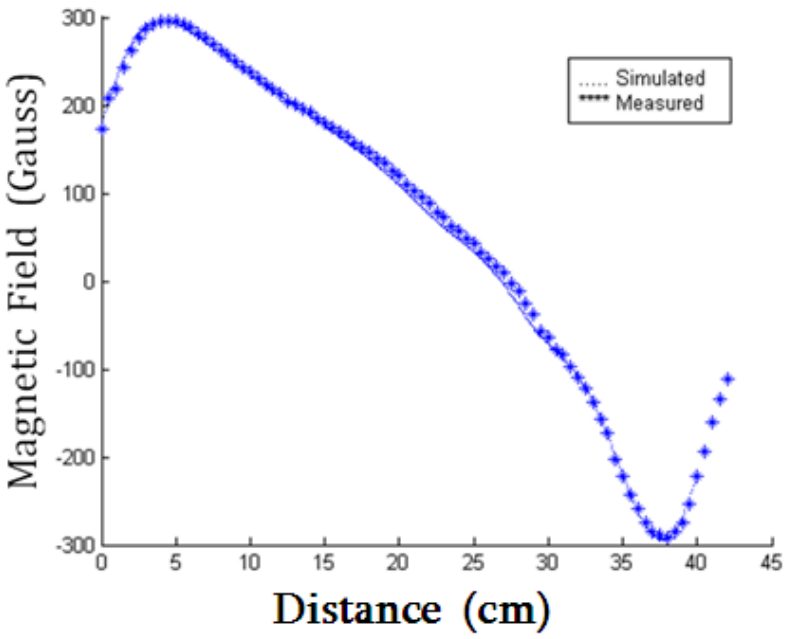

Figure 4.1: Measured magnetic field

The field profile measured matched the simulated profile and the theo-

retical profile closely. This shows that the simulation was quite accurate. Without the extra lengths of coil left for modifications if needed, the actual voltages required were calculated to be 6.2 V for the positive section and 3.4 V for the negative section. With these voltages and the lengths of coil needed, the power dissipation in both the coils can be calculated. The positive coil had a power dissipation of 92.6 W and the negative coil 68.9 W, making the total power dissipation 161.6 W.

4.2 Expected Output

The atoms from the oven follow the Maxwell-Boltzmann velocity distribution. At 900 K, the average velocity is 423 m/s. With the present magnetic field, all atoms with velocities below 450 m/s are expected to slow down. The atoms start decelerating considerably when the detuning and the magnetic field match the Doppler shift. Since then, the force acting on them will be maximum, and the atoms slow down in such a way that the above condition is satisfied until the end. Using the expression for force, it is calculated that at the end of the Zeeman Slower, the atoms have a velocity of 29 m/s. In reality, the mean velocity will be around this calculated value. All atoms above the 450 m/s limit do not undergo any significant deceleration. About 40 percent of the total number of atoms coming out the oven can be expected to contribute to the output flux.

Chapter 5

Discussion

5.1 Comparison of the output fluxes

The output flux of the 2D MOT system can be estimated using the model given in Sec. 2.3.2. The pressure and temperature of the vapour cell will be around 10^{-7} Torr and 900 K. The number density at these values can be calculated to be 8×10^{10}. The length and diameter of the cooling volume are taken to be 50 mm and 12 mm respectively (the sizes of the laser beams are usually approximately these values).

The capture velocity of a MOT is around 60 m/s to 70 m/s. From this, the radial capture velocity v_{c0} can be calculated to be around 50 m/s. The critical longitudinal velocity (below which the radial capture velocity is a constant) is found out using the formula $v_{cr} = Lv_{c0}/2d$ to be around 100 m/s. The radial capture velocity as a function of v_z depends on the above two values.

Γ_{trap} which is the loss rate out of the trap will be the inverse of the lifetime of the MOT. The lifetime is of the order of 100 ms making Γ_{trap} $10s^{-1}$. The outcoupling rate from the trapped volume Γ_{out} will be the inverse of the cooling time. The typical cooling time will be of the order of ms, therefore Γ_{out} is around $10^3 s^{-1}$. Γ_{coll} given by $n\sigma < v >$ can be calculated to be 3.67.

Using these above values, the output flux from the 2D MOT system can be expected to be around 10^9 atoms/s.cm^2. The output flux from a Zeeman Slower is usually around 10^8 atoms/s.cm^2 or a little higher. The flux from a 2D MOT system can exceed that of a Zeeman Slower.

5.2 Zeeman Slower vs. 2D MOT system

The Zeeman Slower and the 2D MOT system each have their own advantages and disadvantages. Even though they operate on different principles, a few factors and experimental aspects of both the systems can be compared.

5.2.1 Zeeman Slower

Advantages

1. The set-up of the Zeeman slower is fairly easy to achieve with a laser beam pointed into a tube to provide a retarding force and coils wound around the tube producing a magnetic field to keep the atomic transition in tune with the laser frequency.

2. Only one beam of laser is needed to provide retarding force as the atoms coming out of the oven are already collimated to a certain extent. This reduces the laser power needed for the source of collimated slow atoms.

3. This system is quite efficient as it slows down more than one-third of the atoms coming out of the oven.

4. The mean speed of the atoms coming out of the Slower is quite low (less than 30 m/s) and the variance of the speeds of the atoms in the collimated beam is not significant.

Disadvantages

1. The detuning required of the laser beam is calculated to be 3.1 GHz. This is an order of magnitude more than what is usually needed and will result in a major loss of laser power as the beam is sent through the required number of acousto-optic modulators.

2. The magnetic field required starts at about 300 G at the ends of both the positive and negative sections of the slower. The coils should carry a high current (15 A and 20 A). The resulting power dissipation (160 W) is too high for the slower to be left without external forced cooling.

3. The atomic beam coming out of the slower has a significant divergence resulting from the spontaneous emission of photons and this would affect the number density and loading rate of the MOT.

4. High vacuum 10^{-10} Torr has to be maintained throughout the tube from the UHV cell to a chamber connecting the slower and the oven. This requires many pumps and a lot of power expended on the pumping system.

5. The Zeeman Slower occupies a lot of space on the set-up table.

5.2.2 2D MOT system

Advantages

1. The set-up is quite compact as the 2D MOT vapour cell is connected to the UHV chamber through only a differential pumping tube. It requires much lesser space than a Zeeman Slower tube.

2. The magnetic field required is quite weak and does not need high current through the four coils surrounding the vapour cell. The field is only to provide a zero field axis and a gradient surrounding it.

3. The atomic beam coming out of the pumping tube into the UHV chamber is very collimated as the aperture into the pumping tube deflects many atoms that have not undergone sufficient cooling to be in the beam.

4. High vacuum is to be maintained only in the UHV chamber. The vapour cell needs to at a vacuum at least three orders lesser than that of the UHV chamber. The power needed for the pumping system is significantly lesser.

5. The four beams of the MOT are only slightly red detuned. Not much laser power is wasted in acousto-optic modulators.

6. No separate forced cooling is required for the source of collimated slow atoms into the UHV chamber.

Disadvantages

1. Four laser beams are required to produce a collimated beam of slow atoms. This is a lot of laser power spent on the source as opposed to a Zeeman Slower system which requires only one laser beam.

2. This system is not very efficient as even though it produces a comparable output flux as that of a Zeeman Slower, only a small fraction of atoms that come out of the oven are sent into the UHV chamber.

3. The mean speed of the atoms in the collimated beam ranges from about 30 m/s to even 60 m/s. The variance of the speeds of these atoms is significant as opposed to that of the Zeeman Slower.

5.3 Oven Collimation System

The design of the oven collimation system given in Sec. 2.4 can produce an output flux of about 10^{11} atoms/s.cm^2. The flux through the hole entering the collimating tube is dependent on the pressure and temperature inside the oven and is about 10^{13} atoms/s.cm^2. The area of the hole is around 0.75 sq.cm.

Another design that can be implemented in the collimation system is the use of a bunch of needles in place of the tube coming out of the oven. The diameter of a needle is 200 μm and the length is about 3 cm. The area of each hole is 3×10^{-4} sq.cm. The two ends of the needles are cut off to make them into capillary tubes. These tubes are placed in the hole out of the oven. The atoms enter the needles or even the spaces between the needles and exit as many collimated streams. This collimation system is expected to be much more effective than the one discussed in Sec. 2.4 as the divergence of the streams coming out of each tube is only about 0.0067 rad which is nearly one-tenth of that of the previous system. These beams travel much further without spreading out significantly. This implies that the fraction of atoms lost at each collimating slit is much lesser than that in the other system.

Another advantage is that as the divergence of each beam depends only on the dimensions of the tube, the hole out of the oven can be much larger in this system. For estimating the fllux out of the oven with this system, we take the diameter of the hole to be 4 cm. The area is about 12 sq.cm. This is more than an order larger than the area that can be taken in the previous system. Combined with the lesser loss of atoms at the collimation slits (due to the lesser divergence), we can estimate the flux out of the oven to be 1 or 2 orders higher than the flux out of the other design i.e. 10^{12} or even 10^{13} atoms/s.cm^2.

5.4 Future Plan

The production of the required magnetic field profile with a solenoid is one half of the work needed to construct a Zeeman Slower. The other half is the laser beam trained into the Slower tube. We need a laser light source of wavelength 461 nm. The plan for the immediate future is to produce a laser beam of wavelength 461 nm by using a laser source of 922 nm and passing it through a nonlinear crystal to let it undergo frequency doubling. As the frequency of the light is doubled in the crystal, the wavelengh reduces to one half which will be 461 nm in this case. A laser source of 461 nm wavelength is necessary for either of the two techniques to produce a collimated beam of slow atoms (a Zeeman Slower or a pure 2D MOT system).

Once a cloud of ultracold Strontium atoms is achieved (after trapping atoms in a 3D MOT followed by a magnetic or dipole trap and evaporative cooling), the atoms are to be placed in a 3D optical lattice to construct a Strontium optical lattice clock. The $^1S_0$- $^3P_0$ transition in these atoms will be probed to count the number of oscillations and thereby measure time.

References

[1] D. Wineland and H. Dehmelt, "Proposed10^{14} $\delta\nu/\nu$ laser fluorescence spectroscopy on TI^{+} mono-ion oscillator", *Bull. Am. Phys. Soc* **20** (1975).

[2] T. Hänsch and A. Schawlow, "Cooling of gases by laser radiation", *Optics Communications* **13**(1), 68 (1975). URL `http://www.sciencedirect.com/science/article/pii/0030401875901595`.

[3] W. D. Phillips and H. Metcalf, "Laser deceleration of an atomic beam", *Phys. Rev. Lett.* **48**, 596 (1982). URL `http://link.aps.org/doi/10.1103/PhysRevLett.48.596`.

[4] S. Chu and C. Wieman, "Laser cooling and trapping of atoms", *J. Opt. Soc. Am. B* **6**, 2020,2020 (1989).

[5] P. Meystre and S. Stenholm, "The mechanical effects of light", *J. Opt. Soc. Am. B* **2**, 1705 (1985).

[6] V. S. Bagnato, G. P. Lafyatis, A. G. Martin, E. L. Raab, R. N. Ahmad-Bitar, and D. E. Pritchard, "Continuous stopping and trapping of neutral atoms", *Phys. Rev. Lett.* **58**, 2194 (1987). URL `http://link.aps.org/doi/10.1103/PhysRevLett.58.2194`.

[7] J. Prodan and W. Phillips, "Chirping the light fantastic - recent NBS atom cooling experiments", *Prog. Quant. Elect* **8** (1984).

[8] W. Ertmer, R. Blatt, J. L. Hall, and M. Zhu, "Laser manipulation of atomic beam velocities: Demonstration of stopped atoms and velocity reversal", *Phys. Rev. Lett.* **54**, 996 (1985). URL `http://link.aps.org/doi/10.1103/PhysRevLett.54.996`.

[9] R. Watts and C. Wieman, "Manipulating atomic velocities using diode lasers", *Opt. Lett* **11** (1986).

[10] J. Dalibard and W. Phillips, "Stability and damping of radiation pressure traps", *Bull. Am. Phys. Soc* **30** (1985).

[11] S. Chu, L. Hollberg, J. E. Bjorkholm, A. Cable, and A. Ashkin, "Three-dimensional viscous confinement and cooling of atoms by resonance radiation pressure", *Phys. Rev. Lett.* **55**, 48 (1985). URL `http://link.aps.org/doi/10.1103/PhysRevLett.55.48`.

[12] P. Lett, R. Watts, C. Tanner, Rolston, Phillips, and Westbrook, "Optical molasses", *J. Opt. Soc. Am. B* **6**, 2084 (1989).

[13] D. Sesco, C. Fan, and C. Wieman, "Production of a cold atomic vapour using diode-laser cooling", *J. Opt. Soc. Am. B* **5** (1988).

[14] J. Dalibard and C. Cohen-Tannoudji, "Laser cooling below the doppler limit by polarization gradients - simple theoretical models", *J. Opt. Soc. Am. B* **6**, 2058 (1989).

[15] T. Udem, J. Reichert, R. Holzwarth, and T. W. Hänsch, "Absolute optical frequency measurement of the cesium D_1 line with a mode-locked laser", *Phys. Rev. Lett.* **82**, 3568 (1999). URL `http://link.aps.org/doi/10.1103/PhysRevLett.82.3568`.

[16] H. Katori, T. Ido, and M. Kuwata-Gonokami, "Optimal design of dipole potentials for efficient loading of Sr atoms", *J. Phys. Soc. Jpn* **68**, 2479 (1999).

[17] H. Katori, M. Takamoto, V. G. Pal'chikov, and V. D. Ovsiannikov, "Ultrastable optical clock with neutral atoms in an engineered light shift trap", *Phys. Rev. Lett.* **91**, 173005 (2003). URL `http://link.aps.org/doi/10.1103/PhysRevLett.91.173005`.

[18] M. Takamoto and H. Katori, "Spectroscopy of the $^1S_0$-$^3P_0$ clock transition of ^{87}Sr in an optical lattice", *Phys. Rev. Lett.* **91**, 223001 (2003). URL `http://link.aps.org/doi/10.1103/PhysRevLett.91.223001`.

[19] M. Takamoto, F. Hong, R. Higashi, and H. Katori, "An optical lattice clock", *Nature* **435**, 321.

[20] R. Le Targat, X. Baillard, M. Fouche, A. Brusch, O. Tcherbakoff, G. D. Rovera, and P. Lemonde, "Accurate optical lattice clock with ^{87}Sr atoms", *Phys. Rev. Lett.* **97**, 130801 (2006). URL `http://link.aps.org/doi/10.1103/PhysRevLett.97.130801`.

[21] A. D. Ludlow, M. M. Boyd, T. Zelevinsky, S. M. Foreman, S. Blatt, M. Notcutt, T. Ido, and J. Ye, "Systematic study of the ^{87}Sr clock transition in an optical lattice", *Phys. Rev. Lett.* **96**, 033003 (2006). URL `http://link.aps.org/doi/10.1103/PhysRevLett.96.033003`.

[22] H. Marion, F. Pereira Dos Santos, M. Abgrall, S. Zhang, Y. Sortais, S. Bize, I. Maksimovic, D. Calonico, J. Gunert, C. Mandache, P. Lemonde, G. Santarelli, P. Laurent, A. Clairon, and C. Salomon, "Search for variations of fundamental constants using atomic fountain clocks", *Phys. Rev. Lett.* **90**, 150801 (2003). URL `http://link.aps.org/doi/10.1103/PhysRevLett.90.150801`.

[23] S. Blatt, A. D. Ludlow, G. K. Campbell, J. W. Thomsen, T. Zelevinsky, M. M. Boyd, J. Ye, X. Baillard, M. Fouche, R. Le Targat, A. Brusch, P. Lemonde, M. Takamoto, F.-L. Hong, H. Katori, and V. V. Flambaum, "New limits on coupling of fundamental constants to gravity using ^{87}Sr optical lattice clocks", *Phys. Rev. Lett.* **100**, 140801 (2008). URL `http://link.aps.org/doi/10.1103/PhysRevLett.100.140801`.

[24] C. Foot. *Atomic Physics* (Oxford, 2005).

[25] Z. T. Lu, K. L. Corwin, M. J. Renn, M. H. Anderson, E. A. Cornell, and C. E. Wieman, "Low-velocity intense source of atoms from a magneto-optical trap", *Phys. Rev. Lett.* **77**, 3331 (1996). URL `http://link.aps.org/doi/10.1103/PhysRevLett.77.3331`.

[26] E. Riis, D. S. Weiss, K. A. Moler, and S. Chu, "Atom funnel for the production of a slow, high-density atomic beam", *Phys. Rev. Lett.* **64**, 1658 (1990). URL `http://link.aps.org/doi/10.1103/PhysRevLett.64.1658`.

[27] K. Dieckmann, R. J. C. Spreeuw, M. Weidemüller, and J. T. M. Walraven, "Two-dimensional magneto-optical trap as a source of slow atoms", *Phys. Rev. A* **58**, 3891 (1998). URL `http://link.aps.org/doi/10.1103/PhysRevA.58.3891`.

[28] J. Schoser, A. Batar, R. Low, V. Schweikhard, A. Grabowski, Y. B. Ovchinnikov, and T. Pfau, "Intense source of cold Rb atoms from a pure two-dimensional magneto-optical trap", *Phys. Rev. A* **66**, 023410 (2002). URL `http://link.aps.org/doi/10.1103/PhysRevA.66.023410`.

[29] F. Reif. *Fundamentals of Statistical and Thermal Physics* (Mc Graw Hill, 1965).

[30] W. M. Haynes. *CRC Handbook of Chemistry and Physics* (CRC Press, 2012).

[31] Z. Ji-Cai, Z. Zun-Lue, L. yu Fang, and S. Jin-Feng, "Elastic scattering properties of untracold strontium atoms", *Chin. Phys. Lett.* **28** (2011).